JLR RESEARCH ARTICLE

Serum opacity factor normalizes erythrocyte morphology in Scarb1$^{-/-}$ mice in an HDL-free cholesterol-dependent way

Ziyi Wang[1,2], **Dedipya Yelamanchili**[1], **Jing Liu**[1,3], **Antonio M. Gotto Jr.**[1,4], **Corina Rosales**[1,4], **Baiba K. Gillard**[1,4,‡], and **Henry J. Pownall**[1,4,*,‡]

[1]Center for Bioenergetics, Houston Methodist, Houston, TX, USA; [2]Departments of Endocrinology and Xiangya Hospital, and [3]Departments of Endocrinology and Cardiovascular Medicine, Xiangya Hospital, Central South University, Changsha, China; [4]Department of Medicine, Weill Cornell Medicine, New York, NY, USA

Abstract Compared with WT mice, HDL receptor-deficient (Scarb1$^{-/-}$) mice have higher plasma levels of free cholesterol (FC)-rich HDL and exhibit multiple pathologies associated with a high mol% FC in ovaries, platelets, and erythrocytes, which are reversed by lowering HDL. Bacterial serum opacity factor (SOF) catalyzes the opacification of plasma by targeting and quantitatively converting HDL to neo HDL (HDL remnant), a cholesterol ester-rich microemulsion, and lipid-free APOA1. SOF delivery with an adeno-associated virus (AAV$_{SOF}$) constitutively lowers plasma HDL-FC and reverses female infertility in Scarb1$^{-/-}$ mice in an HDL-dependent way. We tested whether AAV$_{SOF}$ delivery to Scarb1$^{-/-}$ mice will normalize erythrocyte morphology in an HDL-FC-dependent way. We determined erythrocyte morphology and FC content (mol%) in three groups—WT, untreated Scarb1$^{-/-}$ (control), and Scarb1$^{-/-}$ mice receiving AAV$_{SOF}$—and correlated these with their respective HDL-mol% FC. Plasma-, HDL-, and tissue-lipid compositions were also determined. Plasma- and HDL-mol% FC positively correlated across all groups. Among Scarb1$^{-/-}$ mice, AAV$_{SOF}$ treatment normalized reticulocyte number, erythrocyte morphology, and erythrocyte-mol% FC. Erythrocyte-mol% FC positively correlated with HDL-mol% FC and with both the number of reticulocytes and abnormal erythrocytes. AAV$_{SOF}$ treatment also reduced FC of extravascular tissues to a lesser extent. HDL-FC spontaneously transfers from plasma HDL to cell membranes. AAV$_{SOF}$ treatment lowers erythrocyte-FC and normalizes erythrocyte morphology and lipid composition by reducing HDL-mol% FC.

Supplementary key words cholesterol • HDLs • hyperalphalipoproteinemia • scavenger receptor class B member 1 • atherosclerosis • erythrocyte morphology

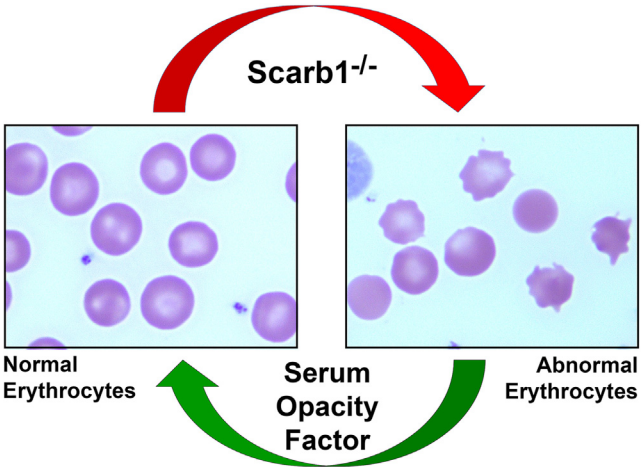

Lipids—free cholesterol (FC), cholesteryl esters (CEs), phospholipids (PLs), and triglycerides (TGs)—are essential components of some cell types and all mammalian plasma lipoproteins. FC is a precursor to steroid hormones, bile acids, and vitamin D. CE and TG, which are produced via the esterification-mediated detoxification of FC and nonesterified fatty acids, form distinct near-homogeneous domains in lipoproteins and lipid droplets within cells. In lipoproteins and the plasma membranes of cells, PLs, the essential FC "solvent," form surface monolayers and bilayer membranes, respectively, that surround neutral lipids in lipoproteins and the cytoplasm and lipid droplets of living cells. Many human diseases are associated with perturbations in the lipid compositions of cells and plasma lipoproteins, including disorders of lipid metabolism (1) and infectious diseases (2, 3). Plasma and tissue lipid compositions are frequently altered by changes in the expression and structures of proteins associated with lipid metabolism. Deficiencies in lecithin-cholesterol acyltransferase (4), the major FC-esterifying activity in mammalian plasma, the low (5) and HDL receptors (6), and lipolytic enzymes in plasma (7) and peripheral tissue (8) are associated with profound phenotypes (9–13).

‡Shared senior authorship.
*For correspondence: Henry J. Pownall, hjpownall@houstonmethodist.org.

 https://doi.org/10.1016/j.jlr.2023.100456

Serum opacity factor (SOF) is a bacterial virulence factor that has an unprecedented activity and mechanism. SOF disrupts HDL structure by releasing lipid-free APOA1 and a small remnant neo HDL, with the concurrent coalescence of nearly all the neutral lipids of >100,000 HDL particles into a CE-rich microemulsion (CERM) that contains APOE and its dimer with APOA2 as its sole apolipoproteins (14, 15). The products of the SOF reaction against HDL support reverse cholesterol transport (i.e., the transfer of peripheral tissue FC to the liver for metabolism (16–19) and disposal) (20). Infusion of low-dose (4 μg) SOF into WT mice reduces their plasma cholesterol by ~40% (21).

In mice, SR-B1, the HDL receptor (scavenger receptor class B member 1) is encoded by Scarb1. Mice deficient in this gene (Scarb1$^{-/-}$) have very high plasma concentrations of FC-rich HDL (22–25), which produce a state of high HDL-FC bioavailability (HDL-FCBI) (25, 26), which is formulated in the Materials and Methods section. FCBI has been described as "active" or accessible cholesterol or, physicochemically as fugacity, an escape tendency analogous to that of the evaporation of a liquid (27–32). The state of high FCBI, mostly as HDL-FC, among Scarb1$^{-/-}$ mice increases the FC content of some but not all tissues (25). Elevated tissue-FC among Scarb1$^{-/-}$ mice is associated with pathologies in heart (33), the arterial wall (atherosclerosis) (23, 34), erythrocytes (altered morphology) (25, 35, 36), adrenals (37), thymocytes (38), and ovaries, which underlies the infertility observed among female Scarb1$^{-/-}$ mice (39–41). Tissues spared the effects of excess FC—brain, kidney, and spleen—do not exhibit any overt pathologies. The magnitude of FC transfer from the HDL of Scarb1$^{-/-}$ versus WT mice to macrophages is higher (+300%) likely explaining atherosclerosis in these mice (25).

Given the profound effects of a high plasma HDL-FCBI among Scarb1$^{-/-}$ mice on cellular tissue cholesterol content and the observations that SOF infusion reduces plasma HDL concentrations in mice and its expression rescues fertility in female Scarb1$^{-/-}$ mice (42), we tested the hypothesis that adeno-associated viral delivery of SOF (AAV$_{SOF}$) to Scarb1$^{-/-}$ mice will reduce the constitutively high tissue and cellular FC contents of Scarb1$^{-/-}$ mice and normalize erythrocyte FC content and morphology.

MATERIALS AND METHODS

Formulation of FCBI

Given that FC and its solvent PL are confined to the same compartments in membranes and lipoproteins, we defined HDL-FCBI according to Equation 1 (26).

$$\text{HDL-FCBI} = \text{HDL-P} \times \text{HDL-mol\% FC} \quad (1)$$

where HDL-P is the HDL particle number, and

$$\text{HDL-mol\% FC} = 100 \times N_{FC}/(N_{FC} + N_{PL}) \quad (2)$$

where N_{FC} and N_{PL} are the moles of FC and PL, respectively. According to Equation 1, a high HDL-P and high HDL-mol% FC underlies a high HDL-FC escape tendency, which increases the amount of FC transfer to other sites—tissues and cells.

Mouse management

All animal studies were approved by the Institutional Animal Use and Care Committee at the Houston Methodist Research Institute. Scarb1$^{-/-}$ and WT C57BL/6J mice (strain no.: 003379 and 000664, respectively; Jackson Laboratory) were maintained on normal laboratory diet (Teklad Envigo; catalog no.: 2920). Mice were periodically genotyped to confirm genetic fidelity; expression of the targeted and WT Scarb1 alleles was confirmed by PCR amplification of DNA extracted from ear punches (primers 5′-GAT-GGG-ACA-TGG-GAC-ACG-AAG-CCA-TTCT-3′ and 5′-TCT-GTC-TCC-GTC-TCC-TTC-AGG-TCC-TGA-3′). All studies were conducted in male and female mice at 12–25 weeks of age except those analyzed for adrenal lipid compositions, which were 8–40 weeks old. Numbers of mice used for the various analyses are given in the legends to figures. We correlated plasma, tissue, and erythrocyte lipid compositions and erythrocyte morphology in three groups of male and female mice—WT, Scarb1$^{-/-}$, and Scarb1$^{-/-}$ mice receiving AAV$_{SOF}$.

AAV$_{SOF}$ treatment

Recombinant SOF, an 80 kDa truncated protein containing full opacification activity, was expressed and isolated from a bacterial expression system as previously described (14, 15). The development of an AAV$_{SOF}$ and its use for treatment of mice has also been described (42). AAV$_{SOF}$ markedly reduces plasma total cholesterol (TC) and HDL-C levels, whereas the control plasmid AAV$_{GFP}$ does not (42). Male and female Scarb1$^{-/-}$ mice aged 12–13 weeks were treated with AAV$_{SOF}$ by intraperitoneal injection at the rate of 1.2×10^{11} genome copies/mouse. Mice were euthanized 3 weeks after AAV$_{SOF}$ injection.

Tissue lipid extraction

Mice were euthanized, and their blood was collected by heart puncture into EDTA; tissues were perfused with PBS and harvested for lipid and protein analyses (18, 21, 43). Tissues were weighed, homogenized, and extracted (hexane:2-propanol:acetic acid = 3:2:1% v/v/v) (43). Tissue-protein was solubilized with 0.4 M NaOH + 1% sodium dodecyl sulfate. Extracted lipids were dissolved in 1% Triton in chloroform, the chloroform was evaporated under nitrogen, and the lipids were solubilized in water for analysis. Compositions were expressed as lipid mass/protein mass. Previously published compositional data for WT and Scarb1$^{-/-}$ mice (25) are included with additional WT and Scarb1$^{-/-}$ mice data and data from the AAV$_{SOF}$-treated mice.

Lipoprotein isolation

Lipoproteins were isolated from pooled mouse plasma (5–10/genotype) by sequential flotation (44, 45). Purity was verified by size-exclusion chromatography (20) and compositional analyses. HDL from individual mice was isolated by heparin-manganese precipitation of plasma APOB lipoproteins (46, 47). Plasma and tissue lipids were determined using enzyme-based assays for FC, TC, PL, and TG (Fujifilm Wako Diagnostics, Inc). Cholesteryl ester (CE) concentrations were calculated as (mg TC − mg FC) × 1.6. When TC and FC are

essentially equal, a small experimental error in the quantitative assay for TC or FC can result in a negative value for the CE and a ratio FC/TC >1.0. We show the data as calculated and did not set all negative CE values as zero values in order to obtain a valid standard deviation for the dataset. Protein was determined by the DC Protein Assay (Bio-Rad, Inc).

Erythrocyte analysis

Blood was collected into EDTA by heart puncture. For lipid analysis, blood was centrifuged to sediment erythrocytes, which were washed and collected, and extracted for lipids as described above. Aliquots of whole blood were used to prepare blood smears for morphological analysis according to the vendor protocol (Sigma Aldrich; catalog no.: 620-75) as follows: blood (1–3 μl) was smeared onto a clean microscope slide, air dried, and fixed with absolute methanol for 2 min. Slides were immersed in Wright Stain (catalog no.: 740) for 4 min and modified Giemsa stain (catalog no.: 620) for 8 min, rinsed two times, 1 min each, air dried at room temperature, and fixed with a drop of HistoChoice Mounting Media (Amresco; catalog no.: H157) under a cover slip. Slides were examined under a microscope (100× oil immersion objective), and individual cells, classified as reticulocytes, normal erythrocytes, or abnormal erythrocytes (acanthocytes), were counted. Calculated percent abnormal cells and reticulocytes are the average scores of two blinded observers who viewed the same slides.

Statistical analysis

Data are presented in the figures as individual values, with mean ± SD, in bar graphs (Sigma Plot 12, Systat Software, Inc.) and correlation plots (Prism 9). Group means were compared by one-way ANOVA with Tukey comparison of means (Prism 9, GraphPad Software, LLC). Linear regression analyses were done using Prism 9. Differences in the plasma, lipoprotein, and tissue lipid compositions of WT versus Scarb1$^{-/-}$ mice with and without treatment with AAV$_{SOF}$ were identified by Tukey comparison of means. Because our previous work (25) showed that the lipid compositions of plasma, plasma lipoproteins, and multiple tissue sites of WT and Scarb1$^{-/-}$ mice differed between sexes for some tissues (25), male and female mice were analyzed separately. For comparisons of genotypes and treatment, the bar graphs show the statistical P values within the same sex, that is, WT-female versus Scarb1$^{-/-}$ female and Scarb1$^{-/-}$ female treated with AAV$_{SOF}$, and WT-male versus Scarb1$^{-/-}$ male and Scarb1$^{-/-}$ male treated with AAV$_{SOF}$. Previous WT and Scarb1$^{-/-}$ data have been included for comparison with our new data on WT, Scarb1$^{-/-}$, and Scarb1$^{-/-}$AAV$_{SOF}$-treated mice. Differences between males and females of the same genotype or treatment are given in the figure legends when significant ($P < 0.05$).

RESULTS

Plasma and HDL lipids

Plasma- and HDL-TC, FC, and CE were higher among both male and female Scarb1$^{-/-}$ versus WT mice but reduced in Scarb1$^{-/-}$ mice receiving AAV$_{SOF}$ (**Fig. 1**A, D, G, J). Plasma- and HDL-PL were less affected by genotype and SOF treatment. In contrast, HDL-TG was not different among the three genotypes but, notably, plasma TG concentrations among Scarb1$^{-/-}$ mice receiving AAV$_{SOF}$ were higher than those WT and untreated Scarb1$^{-/-}$ mice (males only). Both the mol% FC and the FC/TC were higher in the Scarb1$^{-/-}$ versus WT mice but reduced in the former by AAV$_{SOF}$ delivery (Fig. 1B, C, E, F, H, I, K, L). Plasma- and HDL-mol% FC highly correlated and increased as WT ~ Scarb1$^{-/-}$AAV$_{SOF}$ < Scarb1$^{-/-}$ (Fig. 1M, N). Plasma- and HDL-FC also correlated and increased similarly (supplemental Fig. S1). The strength of these correlations is reflected in the slopes (m) of the curves, which for HDL-mol% FC versus plasma-mol% FC are 0.65 and 0.94 for females and males, respectively, at or near unity, with $P < 0.0001$ for both.

Erythrocyte lipids

The lipid compositions of blood erythrocytes from male and female WT versus Scarb1$^{-/-}$ mice were different (**Fig. 2**A, D). As previously reported (25, 36), the erythrocytes from Scarb1$^{-/-}$ mice were more FC rich than those from WT mice. However, we observed that AAV$_{SOF}$ delivery nearly normalized the erythrocyte-FC contents of both male and female Scarb1$^{-/-}$ mice to near WT values. In spite of the SOF-mediated changes in erythrocyte-FC, erythrocyte-mol% FC (Fig. 2B, E) was not significantly reduced versus Scarb1$^{-/-}$ because of parallel changes in PL and FC contents. Meaningful amounts of CE were not detected in the erythrocytes in any of the mice, so the FC/TC ratios among all mouse erythrocytes were nearly equal to one (Fig. 2C, F). Among both male and female WT mice and Scarb1$^{-/-}$ mice ± AAV$_{SOF}$, HDL-FC content and HDL-mol% FC correlated positively with erythrocyte FC content (Fig. 2G, H). The strength of the correlation is reflected in the slopes of the curves, which are ~0.4 for erythrocyte-mol% FC versus HDL-mol% FC, $P < 0.0001$ and >2 for erythrocyte-FC versus HDL-FC, $P < 0.001$ (supplemental Fig. S2).

Erythrocyte morphology

Given that Scarb1 deletion increases erythrocyte-FC and mol% FC with an attendant disruption of erythrocyte morphology (34–36), we tested whether AAV$_{SOF}$, which normalizes erythrocyte-FC composition, would also normalize erythrocyte morphology according to the number of abnormal cells and reticulocytes observed. Normal mouse reticulocyte counts are ~4%, and the abnormal cell count is a bit lower (36). We found that Scarb1 deletion increased the number of abnormal cells and reticulocytes over the normal range, and that this effect was reversed by delivering AAV$_{SOF}$ to the Scarb1$^{-/-}$ mice (**Fig. 3**A, B). The changes in the number of abnormal cells and reticulocytes induced by Scarb1 ablation and treatment with AAV$_{SOF}$ were positively correlated (Fig. 3C). Moreover, as expected, erythrocyte morphology correlated with mol% FC (Fig. 3D, E) and erythrocyte FC (supplemental Fig. S3).

Tissue lipids

The effects of AAV$_{SOF}$ delivery on the FC content of other tissue sites were less profound than those observed in erythrocytes and sometimes varied

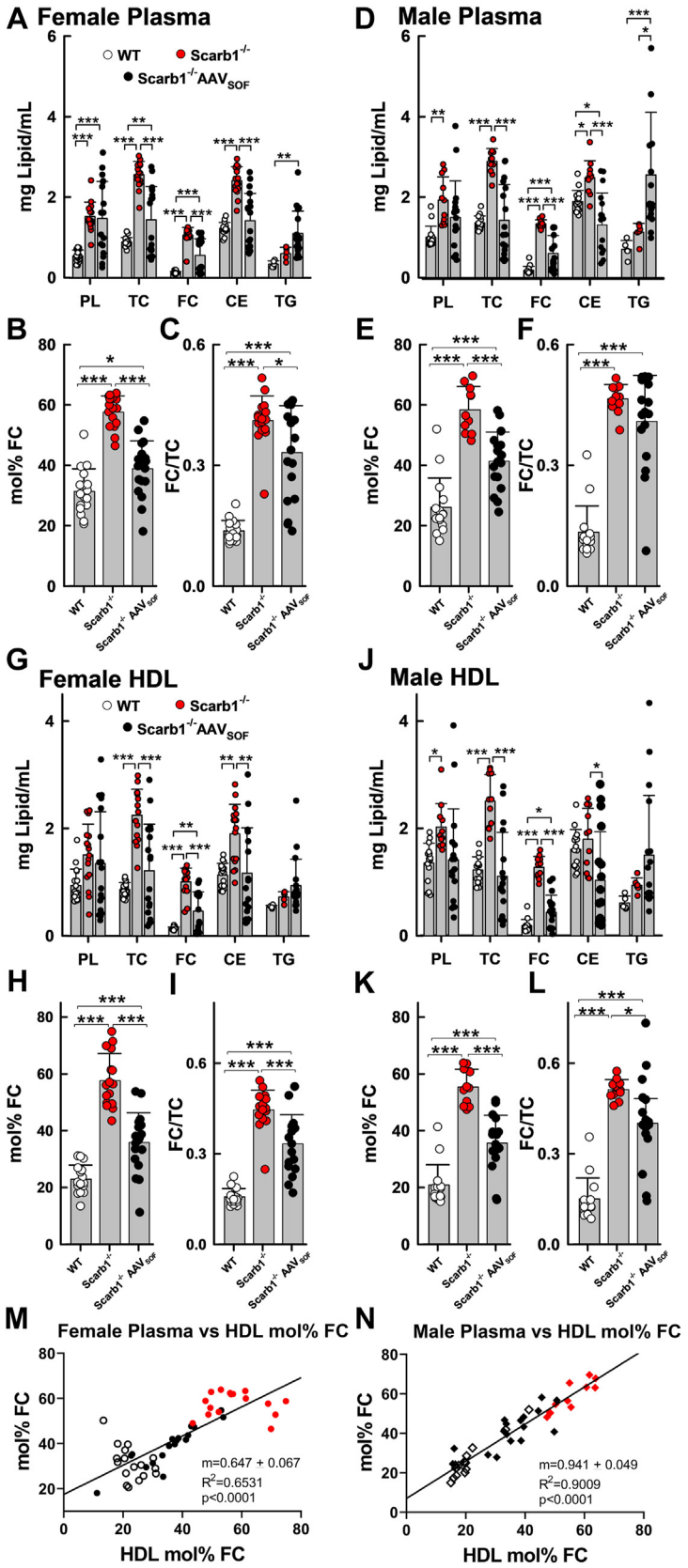

Fig. 1. Plasma and HDL lipid composition. AAV_{SOF} treatment decreases the elevated plasma and HDL TC, FC, CE, mol% FC, and FC/TC levels in Scarb1$^{-/-}$ mice toward WT levels. Plasma (A–F) and HDL (G–L) lipid concentrations of female (left panels) and male (right panels) WT, Scarb1$^{-/-}$, and AAV_{SOF}-treated Scarb1$^{-/-}$ mice. M and N: Plasma and HDL-mol% FC were highly correlated for both females (M) and males (N). HDLs were obtained from individual mouse plasma by heparin-manganese depletion of APOB lipoproteins. Data points are values for individual mice, and bars are mean ± SD. Numbers of female (-F) and male (-M) mice per

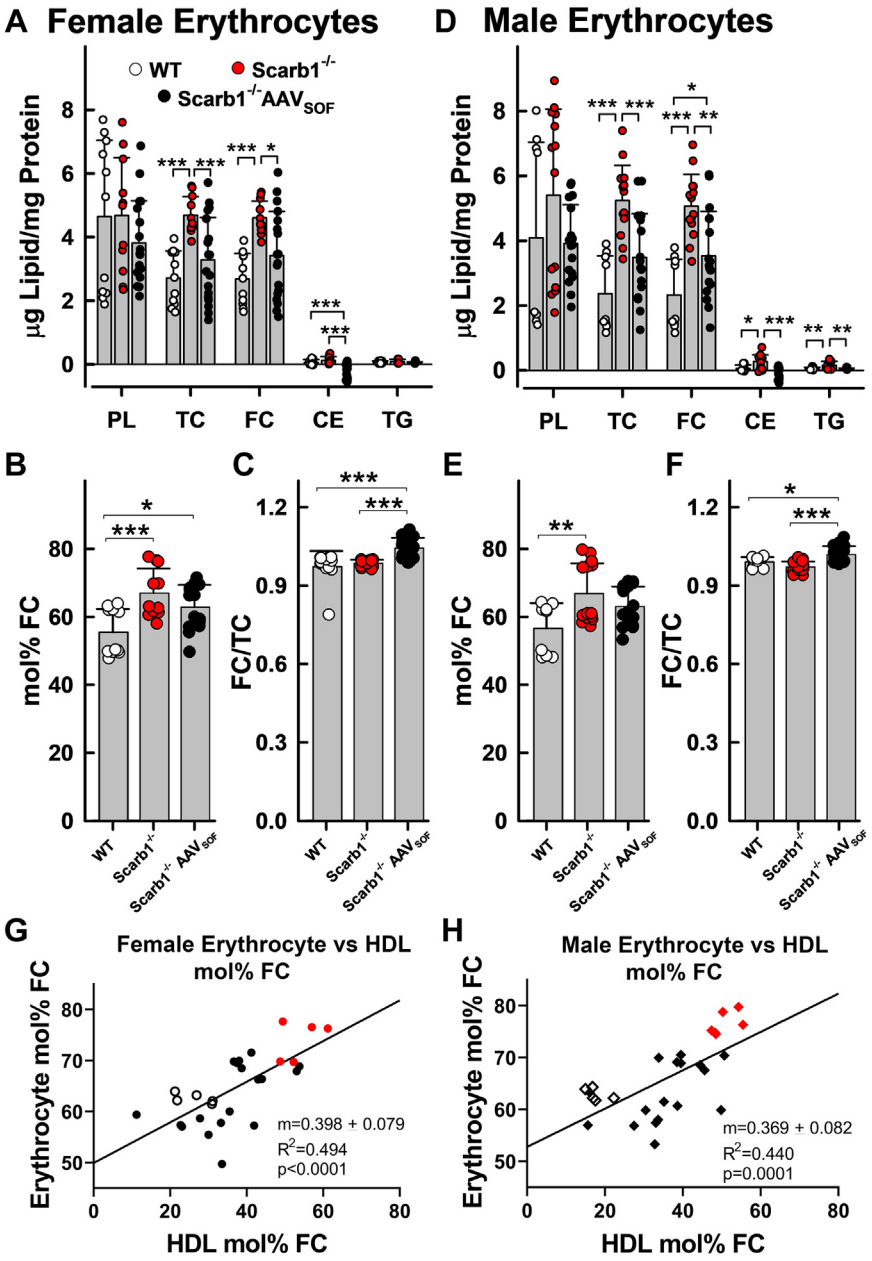

Fig. 2. Erythrocyte lipid composition. AAV_{SOF} treatment decreases the elevated erythrocyte (red blood cell) TC, FC, and mol% FC in Scarb1$^{-/-}$ mice toward WT levels. Panels A–C (female) and D–F (male) provide the lipid composition relative to protein (W/W), mol% FC, and the FC/TC ratio (W/W). G and H: Correlation of erythrocyte versus HDL-mol% FC. Data points are values for individual mice, and bars are mean ± SD. Mice/group for the bar graphs were WT-F (n = 11), Scarb1$^{-/-}$F (n = 11), Scarb1$^{-/-}$F$_{AAVSOF}$ (n = 18), WT-M (n = 9), Scarb1$^{-/-}$M (n = 14), and Scarb1$^{-/-}$M$_{AAVSOF}$ (n = 17) and for the correlation plots WT-F (n = 5), Scarb1$^{-/-}$F (n = 5), Scarb1$^{-/-}$F$_{AAVSOF}$ (n = 18), WT-M (n = 5), Scarb1$^{-/-}$M (n = 6), and Scarb1$^{-/-}$M$_{AAVSOF}$ (n = 17). Statistics are as described in the legend to Figure 1. Comparisons between male and female data within the same genotype or treatment group showed no significant differences between sexes for any of the analytes. Note: Data in the correlation plots are only for those mice from which both plasma and erythrocytes were collected so there are fewer paired values for the correlations (G, H) than the total number of mice in the bar graphs.

group were WT-F (n = 17), Scarb1$^{-/-}$F (n = 16), Scarb1$^{-/-}$F$_{AAVSOF}$ (n = 18), WT-M (n = 15), Scarb1$^{-/-}$M (n = 11), and Scarb1$^{-/-}$M$_{AAVSOF}$ (n = 17). Group means were compared by ANOVA with Tukey comparison of means as described in the Materials and Methods section. P values for significantly different pairwise comparisons (*$P \leq 0.05$, **$P \leq 0.01$, and***$P \leq 0.001$) are indicated over brackets. The slope m, R^2, and P values for the linear regression line for the correlation plots (M, N) are shown on the graphs. Comparisons between male and female data within the same genotype or treatment group for plasma: CE: WT-F < WT-M, $P = 0.0048$; TG: AAV_{SOF}-F < AAV_{SOF}-M, $P = 0.0005$, whereas for HDL, there were no significant differences between sexes for any of the analytes.

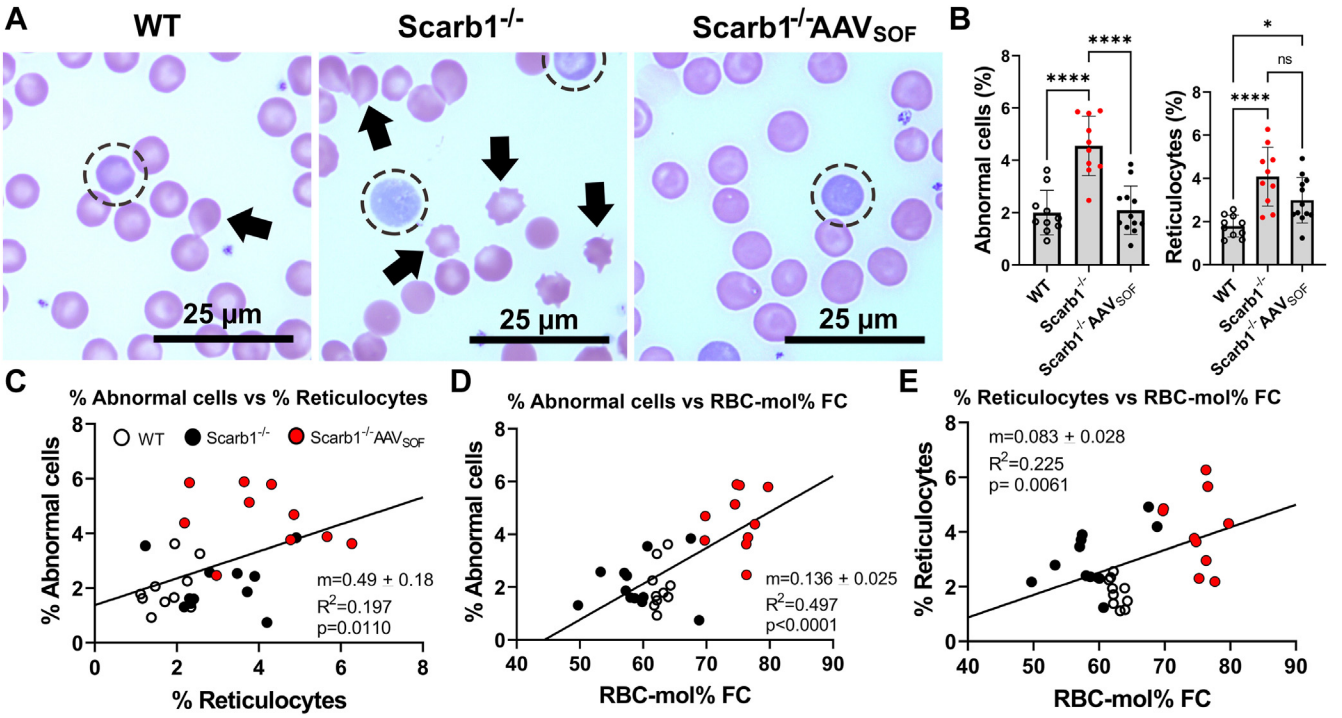

Fig. 3. Erythrocyte (red blood cell [RBC]) morphology correlates with RBC-FC. AAV_{SOF} normalizes both the RBC-FC content and morphology. A: Micrographs of representative fields of blood smears stained with Wright/Giemsa stain from WT, Scarb1$^{-/-}$, and AAV_{SOF}-treated Scarb1$^{-/-}$ mice (Arrows: abnormal cells; circles: reticulocytes). B, quantitation of erythrocyte morphology based on counts of abnormal cells (acanthocytes) and reticulocytes. Data from male and female mice were not significantly different; so pooled data are shown. C: Correlation of percent abnormal cells versus percent reticulocytes. D and E: Correlation of percent abnormal and percent reticulocyte cells with erythrocyte-mol% FC. Mice/group: WT (n = 10), Scarb1$^{-/-}$ (n = 10), and Scarb1$^{-/-}{}_{AAVSOF}$ (n = 12). Data plotted by sex were not different; so male and female data were pooled.

according to sex. FC is elevated in both male and female heart tissue in Scarb1$^{-/-}$ mice, and AAV_{SOF} treatment increased heart-FC and mol% FC in both sexes. However, AAV_{SOF} reduced the FC/TC ratio in males only (**Fig. 4**A–F). Nevertheless, heart-mol% FC significantly and positively correlated with HDL-mol% FC in both males and females (Fig. 4G, H). FC is elevated in lungs of both female and male Scarb1$^{-/-}$ mice (Fig. 4I–P). AAV_{SOF} treatment reduced FC in female lungs but not male lungs. AAV_{SOF} does not reduce elevated mol% FC in either male Scarb1$^{-/-}$ or female Scarb1$^{-/-}$ lungs. The effects of AAV_{SOF} in lung were small, but still lung-mol% FC significantly and positively correlated with HDL-mol% FC (Fig. 4O, P). In liver, AAV_{SOF} normalized the elevated FC content and mol% FC in females but increased the mol% FC in males (Fig. 4Q–S, T–V). AAV_{SOF} failed to reverse the effects of Scarb1 deletion on liver-TG and reduced TG content (Fig. 4Q, T). Female but not male liver-mol% FC correlated with HDL mol% FC (Fig. 4W, X).

Within the steroidogenic tissues, there were some notable effects of AAV_{SOF}. In ovaries, AAV_{SOF} reduced CE content, did not change the FC content, but normalized the PL content, thereby normalizing the mol% FC (**Fig. 5**A, B and Equation 2) but not the FC/TC ratio (Fig. 5C). Ovary-mol% FC correlated with that of HDL-mol% FC (Fig. 5G). Although AAV_{SOF} altered FC and CE content, the mol% FC, and the FC/TC ratio in testes, the effects were small (Fig. 5E–H). Although testes-mol% FC correlated negatively with that of HDL-mol% FC, the effect was also small and not significant. Adrenal TC and CE are reduced in both male and female Scarb1$^{-/-}$ mice. (Fig. 5I–N). The effects of AAV_{SOF} on adrenal lipid composition were small; AAV_{SOF} normalized the mol% FC in males and females (trend) and increased the FC/TC ratio but failed to normalize the profound reduction in CE induced by Scarb1 deletion. Unexpectedly, adrenal-mol% FC correlated negatively with HDL-mol% FC for males ($P = 0.008$) and females (nonsignificant, $P = 0.142$).

In brain, AAV_{SOF} increased FC content, mol% FC, and the FC/TC ratio but reduced CE content; there was no correlation between brain-mol% FC and HDL-mol% FC (supplemental Fig. S4). The effects of AAV_{SOF} on the lipids in the kidney (supplemental Fig. S5), spleen (supplemental Fig. S6), and testes- and ovary-fat (supplemental Fig. S7) were mostly small and not significant except for the paradoxical increase in FC, mol % FC, and TG (>+300%) in testes- and ovary-fat (supplemental Fig. S7A–F). In spleen, the major effect was a reduction in TG content, whereas in kidneys, AAV_{SOF} increased FC content and mol% FC to WT levels only in males. In kidney, spleen, and fat tissues, tissue-mol% FC and HDL-mol% FC were not correlated.

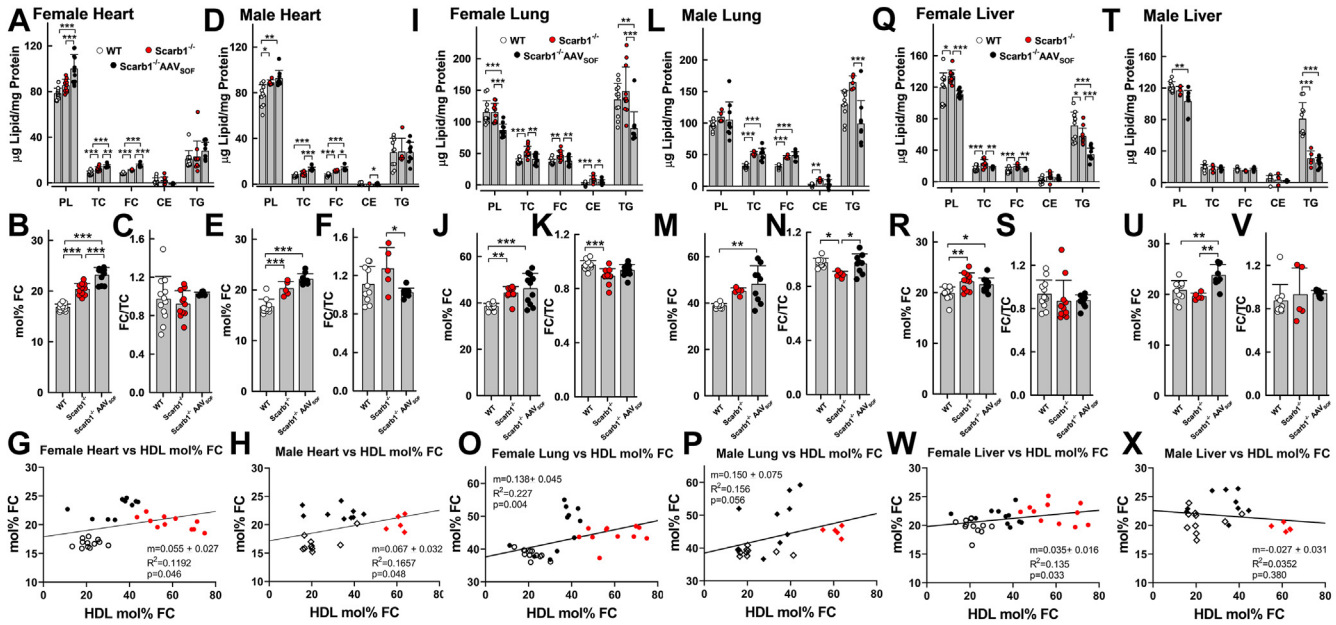

Fig. 4. Heart, lung, and liver lipid composition. AAV_{SOF} treatment has variable effects on the cholesterol content of heart, lung, and liver in Scarb1$^{-/-}$ mice. A–H: Heart; (I–P) Lung; and (Q–X) Liver. The respective panels provide the lipid composition relative to protein (W/W), mol% FC, and the FC/TC ratio (W/W). Data points are values for individual mice, and bars are mean ± SD. Mice/group were WT-F (n = 12), Scarb1$^{-/-}$F (n = 11), Scarb1$^{-/-}$F$_{AAVSOF}$ (n = 11), WT-M (n = 10), Scarb1$^{-/-}$M (n = 5), and Scarb1$^{-/-}$M$_{AAVSOF}$ (n = 9). Statistics are as described in the legend to Figure 1. Comparisons between male and female data within the same genotype or treatment group gave the following significant differences between sexes: heart: TC: Scarb1$^{-/-}$F> Scarb1$^{-/-}$M, P = 0.0137; FC: AAV_{SOF}-F> AAV_{SOF}-M, P = 0.0084; CE: Scarb1$^{-/-}$F> Scarb1$^{-/-}$M, P = 0.0015; FC/TC: Scarb1$^{-/-}$M> Scarb1$^{-/-}$F, P = 0.0025. Lung: TC: AAV_{SOF}-M> AAV_{SOF}-F, P = 0.0286; AAV_{SOF}-M> AAV_{SOF}-F, P = 0.0019. Liver: TC: Scarb1$^{-/-}$F> Scarb1$^{-/-}$M, P = 0.0085; FC: Scarb1$^{-/-}$F> Scarb1$^{-/-}$M, P = 0.0017; TG: Scarb1$^{-/-}$F> Scarb1$^{-/-}$M, P = 0.0074; mol% FC: Scarb1$^{-/-}$F> Scarb1$^{-/-}$M, P = 0.0587 and AAV_{SOF}-M> AAV_{SOF}-F, P = 0.0470. Note: In some instances, the calculated FC/TC ratio was >1 because of the imprecision of some of the analyses at concentrations near the detection limits of the assay.

Sex differences in tissue-lipids and response to AAV_{SOF}

In our previous study of tissue lipids in the Scarb1$^{-/-}$ versus WT mouse (25), we found significant differences between lipid content of males versus females of the same genotype in some of the tissues. In this study, male and female data are presented in separate panels, and male versus female differences are summarized in the figure legends. Response of tissue lipids to AAV_{SOF} treatment also varied by sex. For example, FC is higher in lungs of both female and male Scarb1$^{-/-}$ versus WT mice, but AAV_{SOF} treatment reduces FC to WT levels in female lungs but not male lungs (Fig. 4I, L). In liver, FC is elevated in female Scarb1$^{-/-}$ mice and reduced with AAV_{SOF} treatment, whereas FC in liver of male Scarb1$^{-/-}$ does not differ from WT and is not altered with AAV_{SOF} treatment (Fig. 4Q, T). In kidney, FC in Scarb1$^{-/-}$ females does not differ from WT and is not altered by AAV_{SOF}, whereas FC in Scarb1$^{-/-}$ male mice is lower than in WT mice, and AAV_{SOF} increases FC to WT levels and increases mol% FC in the male mice (supplemental Fig. S6). In spleen, FC is lower in female Scarb1$^{-/-}$ versus WT mice, AAV_{SOF} decreases FC further, but mol% FC is the same in all three groups of female mice. FC is higher in spleens of male Scarb1$^{-/-}$ mice versus WT mice, AAV_{SOF} reduced spleen FC below WT levels and decreased spleen-mol% FC. The correlations between HDL-mol% FC and FC for erythrocytes and all tissues are summarized in supplemental Table S1.

DISCUSSION

HDL receptor deficiency in Scarb1$^{-/-}$ mice leads to the accretion of HDL that is dysfunctional because it occurs at a higher plasma concentration and contains more FC than receptor-competent WT HDL. This creates a state of high FCBI, which has been described as "active cholesterol" and fugacity. We use the term bioavailability because of the biological consequences of FC escape from HDL in vivo. HDL-FC is highly mobile and rapidly clears from plasma in mice ($t_{1/2}$ = 5 min) (48) and humans ($t_{1/2}$ = 9 min) (49) and in mice rapidly transfers to nearly all tissues (48). Whereas FC uptake in some tissues, such as liver, is mediated by SR-B1, transfer to many other tissues, including the intestine, occurs by diffusion, sometimes called transintestinal cholesterol efflux (50). Previous in vitro studies showed that HDL-FC transfer to cells increases with increasing HDL concentration and HDL-FC content (51) so that one would expect more FC to transfer to cells and tissues from HDL of Scarb1$^{-/-}$ versus WT mice. Scarb1$^{-/-}$ mice present with multiple pathologies—female infertility, atherosclerotic cardiovascular

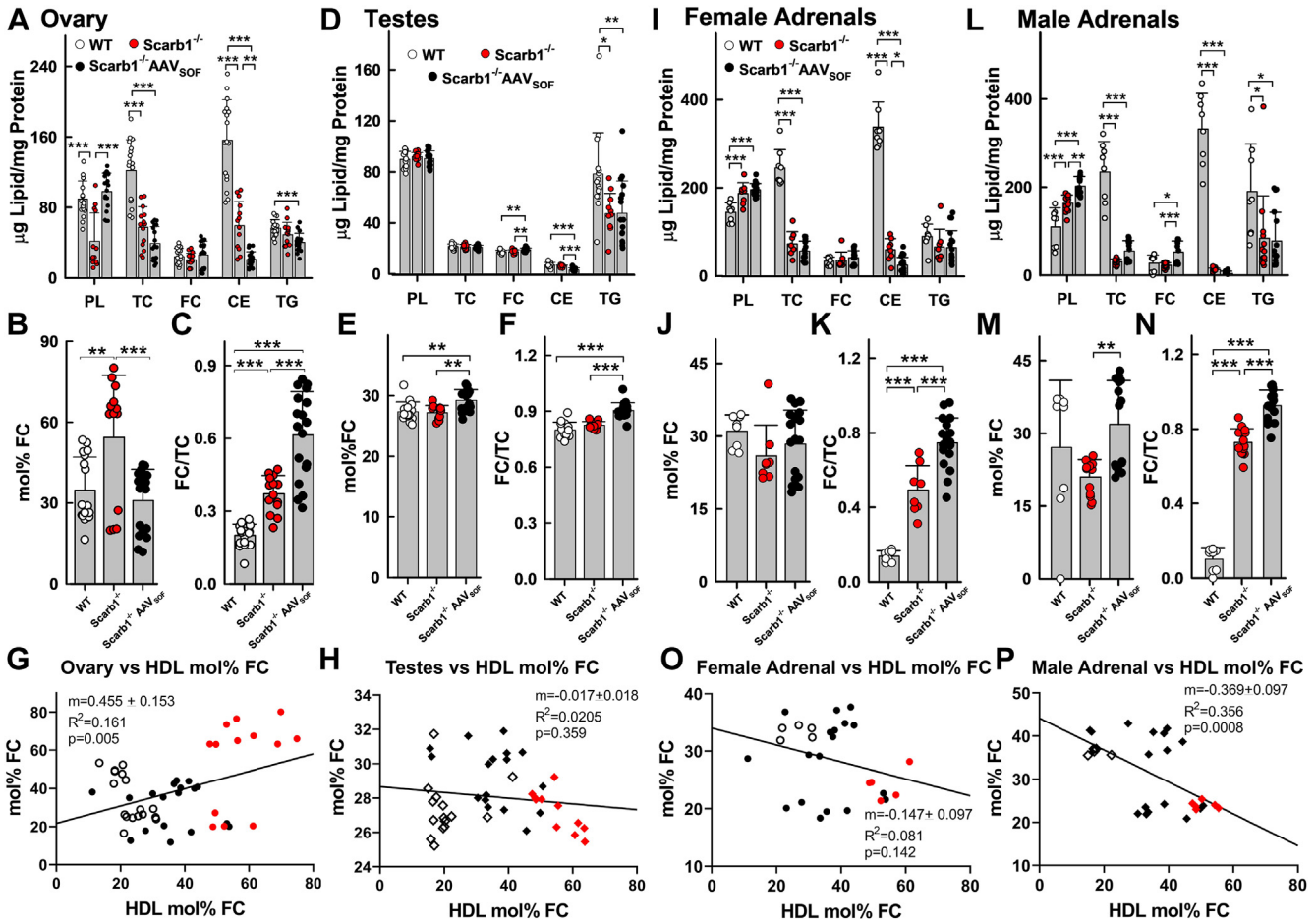

Fig. 5. Steroidogenic tissue lipid composition. AAV_{SOF} treatment decreases the elevated mol% FC to WT levels in ovaries but does not restore the low CE levels of ovaries or adrenals of Scarb1$^{-/-}$ mice. A–C and G: ovary; D–F and H: testis, and I–P: adrenals. The respective panels provide the lipid composition relative to protein (W/W), mol% FC, and the FC/TC ratio (W/W). Data points are values for individual mice, and bars are mean ± SD. Mice/group for ovaries : WT-F (n = 17), Scarb1$^{-/-}$F (n = 14), Scarb1$^{-/-}F_{AAVSOF}$ (n = 18); for testis, WT-M (n = 15), Scarb1$^{-/-}$M (n = 11), and Scarb1$^{-/-}M_{AAVSOF}$ (n = 17); for adrenals: WT-F (n = 5–8), Scarb1$^{-/-}$F (n = 5–8), Scarb1$^{-/-}F_{AAVSOF}$ (n = 18), WT-M (n = 5–8), Scarb1$^{-/-}$M (n = 6–13), and Scarb1$^{-/-}M_{AAVSOF}$ (n = 17). Statistics are as described in the legend to Figure 1. Comparisons between male and female adrenal data within the same genotype or treatment group gave the following significant differences between sexes: CE: Scarb1$^{-/-}$F> Scarb1$^{-/-}$M, $P = 0.0426$; TG: WT-M> WT-F, $P = 0.0473$; FC/TC: Scarb1$^{-/-}$M> Scarb1$^{-/-}$F, $P < 0.0001$ and AAV_{SOF}-M> AAV_{SOF}-F, $P < 0.0001$.

disease, and platelet and erythrocyte abnormalities (34, 36, 39, 52). Some of these effects—erythrocyte abnormalities, (34) atherosclerosis (34), and infertility (39)—are reversed by the HDL-lowering drug, probucol, or by AAV_{SOF} delivery (42). In vitro, SOF activity versus HDL produces lipid-free APOA1 and remnant HDL, but in vivo, these rapidly convert to HDL and are hepatically extracted (17), and the plasma HDL concentration declines. Thus, we tested the hypothesis that AAV_{SOF}-mediated reduction of plasma- and HDL-FC would also normalize lipid composition and morphology of erythrocytes, which are also FC acceptors in other settings, including cholesterol efflux (53).

While WT and Scarb1$^{-/-}$ mice have similar hematocrits, Scarb1$^{-/-}$ mice have greater erythrocyte volumes and lower erythrocyte hemoglobin, and according to filipin staining, the cholesterol content of erythrocytes from Scarb1$^{-/-}$ mice is higher than that of WT mice (36). We quantified this observation using an enzymatic assay and further showed that plasma-, HDL-, and erythrocyte-mol% FC is highest in Scarb1$^{-/-}$ compared with AAV_{SOF}-exposed Scarb1$^{-/-}$ mice and lowest in WT mice. Given that HDL is the major lipoprotein in mice, high HDL-mol% FC underlies the high plasma-mol% FC and is the major source of FC, which in turn drives erythrocyte-mol% FC. The strong correlation is reflected in the slopes of the curves for plasma-mol% FC versus HDL-mol% FC, which are close to unity (Fig. 1M, N). The correlations between erythrocyte-mol% FC versus HDL-mol% FC are equally robust with slopes of 0.40 and 0.37 for females and males, respectively. The slopes are less than unity suggesting that the mol% FC are at steady state but not at equilibrium and that the erythrocyte-mol % FC is less than that of HDL-mol% FC.

FC accretion by erythrocytes is higher than in many other cells or tissues; this occurs for two reasons. First, erythrocytes reside in the same compartment, namely plasma, as the source of excess FC, HDL. Second,

erythrocytes have no metabolic defense against a high FCBI; they lack the intracellular FC-esterifying enzymes and plasma membrane lipid transporters that detoxify or exocytose FC, respectively. Thus, under conditions of high FCBI, erythrocytes, like LDLs (25), which is also confined to the plasma compartment, rapidly ($t_{1/2}$ = ~3 min) accumulate FC (i.e., faster than the rate of FC transfer to the major tissues) (48). Changes in HDL-mol% FC have a greater effect on abnormal cell formation versus reticulocyte production: the effects of an increased HDL-mol% FC on abnormal cell formation were greater (m = 0.136) than its effects on reticulocyte production (m = 0.083; Fig. 3D, E).

A high erythrocyte-FC is associated with an increased number of abnormal erythrocytes, characterized by "blebbing." The erythrocyte-plasma membrane is asymmetric with respect to FC distribution (54–60). One estimate using orthogonal lipid sensors puts the outer leaflet ratio to inner leaflet ratio at ~12 (61). Consistently, most studies observed more FC in the outer versus inner leaflet of the plasma membrane even though the ranges of inner-to-outer leaflet FC vary considerably among studies. This occurs despite FC transfer between leaflets on a millisecond time scale (62). This asymmetry has been attributed the asymmetry in the compositions of the FC-binding PLs. The outer leaflet contains more highly cholesterophilic PL—saturated phosphatidylcholines and especially sphingomyelin (63), whereas, the PLs of the inner leaflet are nearly devoid of sphingomyelin and contain ~80% of the plasma membrane unsaturation (60). As a consequence, under conditions of high FCBI, FC preferentially accumulates in the outer leaflet, and to accommodate the additional FC, blebs form. This structure is maintained because the rates of PL translocation across the plasma membrane are slower than that of FC (62, 64). When the HDL-FC is reduced by either probucol (34) or AAV_{SOF}, the normal structures are restored.

FC also transfers rapidly to liver because it is highly perfused (48). Given that probucol, like SOF, reduces HDL-C concentrations, changes in the tissue lipid compositions induced by SOF may also occur in patients receiving probucol and could underlie some of the metabolic consequences of probucol therapy. The elevation of plasma-TG but not HDL-TG by AAV_{SOF} suggests that some products of the SOF reaction, most likely the CERM, compete with either TG hydrolysis, or, more likely, the CERM produced by the SOF competes with endogenous very LDL uptake by the LDL receptor and other lipoprotein receptors (20). This would be consistent with the observation that in most tissues in which TG was altered, that is, lung, liver, ovaries, and male adrenals, kidney, and spleen, TG in the AAV_{SOF} mice was lower than in the Scarb1$^{-/-}$ control or WT mice. The exceptions were fat tissue surrounding the ovaries and testis, in which the TG was elevated in the AAV_{SOF}-treated mice (supplemental Fig. S7).

Although underlying mechanisms may differ, many lipid disorders are associated with erythrocyte abnormalities; for example, abetalipoproteinemia (65) is caused by mutations in the gene encoding microsomal TG transfer protein (66). In abetalipoproteinemia, the observed acanthacytosis is associated with the absence of LDL and the occurrence of erythrocytes that are phosphatidylcholine poor and SM rich compared with normolipidemic erythrocytes (67). Compared with a normolipidemic cohort, patients with total deficiency of the FC-esterifying enzyme, lecithin-cholesterol acyltransferase, have a high FC/CE ratio and present with hemolytic anemia, in which there is premature erythrocyte hemolysis that results in anemia. Notably, patients with acute coronary syndrome have higher erythrocyte-FC than do those with stable coronary artery disease, and erythrocyte-FC content better predicted acute coronary syndrome than either HDL-C or C-reactive protein levels (68).

Limitations of the study

The Scarb1$^{-/-}$ mouse has an extreme phenotype that has not been documented in humans. Thus, the value of the study is mechanistic, revealing how changes in plasma FC concentrations impact tissue FC content, an effect that was shown to be reversible, in part, by delivering AAV_{SOF} to Scarb1$^{-/-}$ mice.

CONCLUSIONS

HDL-FC spontaneously transfers from plasma lipoproteins to cell membranes in multiple tissue sites on a time scale of minutes to a few hours. FC enrichment of erythrocytes, which are in contact with plasma HDL, was more profound than tissue-FC enrichment. AAV_{SOF} treatment lowers both plasma HDL-FC and erythrocyte-FC and normalizes erythrocyte morphology and lipid composition in an HDL-FC-dependent way. Therapy with an SOF mimetic could be useful for treatment of patients who present with high HDL-C bioavailability as a risk factor for atherosclerotic cardiovascular diseases or other metabolic disorders.

Data Availability

All data are contained within the article.

Supplemental data

This article contains supplemental data.

Acknowledgments

The authors thank Jacob M. Kolman, MA, ISMPP CMPP™ (Houston Methodist Academic Institute) for reviewing and editing the article.

Author contributions

H. J. P. conceptualization; Z. W., D. Y., J. L., and B. K. G. formal analysis; Z. W., D. Y., J. L., A. M. G., and C. R. data

curation; H. J. P. writing–original draft; Z. W., D. Y., J. L., A. M. G., C. R., B. K. G., and H. J. P. writing–review & editing.

Author ORCIDs
Jing Liu https://orcid.org/0000-0002-1019-0843
Antonio M. Gotto https://orcid.org/0000-0001-8076-6783
Corina Rosales https://orcid.org/0000-0002-9068-2775
Baiba K. Gillard https://orcid.org/0000-0002-2527-5102
Henry J. Pownall https://orcid.org/0000-0001-8412-506X

Funding and additional information
This work was supported by the National Institutes of Health (to H. J. P. and C. R.; grant no.: R01-HL149804) and from the Houston Methodist Hospital Foundation (to H. J. P.). The content is solely the responsibility of the authors and does not necessarily represent the official views of the National Institutes of Health.

Conflict of interest
The authors declare that they have no conflicts of interest with the contents of this article.

Abbreviations
AAV, adeno-associated virus; CE, cholesteryl ester; CERM, cholesteryl ester-rich microemulsion; FC, free cholesterol; FCBI, FC bioavailability; PL, phospholipid; Scarb1, scavenger receptor class B, member 1; SOF, serum opacity factor; TC, total cholesterol; TG, triglyceride.

Manuscript received August 9, 2023, and in revised form September 16, 2023. Published, JLR Papers in Press, October 10, 2023, https://doi.org/10.1016/j.jlr.2023.100456

REFERENCES

1. Scriver, R. C. (2001) Metabolic Basis of Inherited Disease. McGraw-Hill, New York
2. Khovidhunkit, W., Kim, M. S., Memon, R. A., Shigenaga, J. K., Moser, A. H., Feingold, K. R., *et al.* (2004) Effects of infection and inflammation on lipid and lipoprotein metabolism: mechanisms and consequences to the host. *J. Lipid Res.* **45**, 1169–1196
3. Courtney, H. S., and Pownall, H. J. (2010) The structure and function of serum opacity factor: a unique streptococcal virulence determinant that targets high-density lipoproteins. *J. Biomed. Biotechnol.* **2010**, 956071
4. Pavanello, C., and Calabresi, L. (2020) Genetic, biochemical, and clinical features of LCAT deficiency: update for 2020. *Curr. Opin. Lipidol.* **31**, 232–237
5. Goldstein, J. L., and Brown, M. S. (2015) A century of cholesterol and coronaries: from plaques to genes to statins. *Cell.* **161**, 161–172
6. Acton, S., Rigotti, A., Landschulz, K. T., Xu, S., Hobbs, H. H., and Krieger, M. (1996) Identification of scavenger receptor SR-BI as a high density lipoprotein receptor. *Science.* **271**, 518–520
7. Goldberg, I. J. (2018) 2017 george lyman duff memorial lecture: fat in the blood, fat in the artery, fat in the heart: triglyceride in physiology and disease. *Arterioscler. Thromb. Vasc. Biol.* **38**, 700–706
8. Zechner, R., Zimmermann, R., Eichmann, T. O., Kohlwein, S. D., Haemmerle, G., Lass, A., *et al.* (2012) FAT SIGNALS-lipases and lipolysis in lipid metabolism and signaling. *Cell Metab.* **15**, 279–291
9. Glomset, J. A., Norum, K. R., and King, W. (1970) Plasma lipoproteins in familial lecithin: cholesterol acyltransferase deficiency: lipid composition and reactivity in vitro. *J. Clin. Invest.* **49**, 1827–1837
10. Goldstein, J. L., and Brown, M. S. (1974) Binding and degradation of low density lipoproteins by cultured human fibroblasts. Comparison of cells from a normal subject and from a patient with homozygous familial hypercholesterolemia. *J. Biol. Chem.* **249**, 5153–5162
11. Zanoni, P., Khetarpal, S. A., Larach, D. B., Hancock-Cerutti, W. F., Millar, J. S., Cuchel, M., *et al.* (2016) Rare variant in scavenger receptor BI raises HDL cholesterol and increases risk of coronary heart disease. *Science.* **351**, 1166–1171
12. Fojo, S. S., and Brewer, H. B. (1992) Hypertriglyceridaemia due to genetic defects in lipoprotein lipase and apolipoprotein C-II. *J. Intern. Med.* **231**, 669–677
13. Steinberg, D. (1978) Elucidation of the metabolic error in Refsum's disease: strategy and tactics. *Adv. Neurol.* **21**, 113–124
14. Courtney, H. S., Zhang, Y. M., Frank, M. W., and Rock, C. O. (2006) Serum opacity factor, a streptococcal virulence factor that binds to apolipoproteins A-I and A-II and disrupts high density lipoprotein structure. *J. Biol. Chem.* **281**, 5515–5521
15. Gillard, B. K., Courtney, H. S., Massey, J. B., and Pownall, H. J. (2007) Serum opacity factor unmasks human plasma high-density lipoprotein instability via selective delipidation and apolipoprotein A-I desorption. *Biochemistry.* **46**, 12968–12978
16. Gillard, B. K., Bassett, G. R., Gotto, A. M., Jr., Rosales, C., and Pownall, H. J. (2017) Scavenger receptor B1 (SR-B1) profoundly excludes high density lipoprotein (HDL) apolipoprotein AII as it nibbles HDL-cholesteryl ester. *J. Biol. Chem.* **292**, 8864–8873
17. Rodriguez, P. J., Gillard, B. K., Barosh, R., Gotto, A. M., Jr., Rosales, C., and Pownall, H. J. (2016) Neo high-density lipoprotein produced by the streptococcal serum opacity factor activity against human high-density lipoproteins is hepatically removed via dual mechanisms. *Biochemistry.* **55**, 5845–5853
18. Gillard, B. K., Rodriguez, P. J., Fields, D. W., Raya, J. L., Lagor, W. R., Rosales, C., *et al.* (2016) Streptococcal serum opacity factor promotes cholesterol ester metabolism and bile acid secretion in vitro and in vivo. *Biochim. Biophys. Acta.* **1861**, 196–204
19. Tchoua, U., Rosales, C., Tang, D., Gillard, B. K., Vaughan, A., Lin, H. Y., *et al.* (2010) Serum opacity factor enhances HDL-mediated cholesterol efflux, esterification and anti inflammatory effects. *Lipids.* **45**, 1117–1126
20. Gillard, B. K., Rosales, C., Pillai, B. K., Lin, H. Y., Courtney, H. S., and Pownall, H. J. (2010) Streptococcal serum opacity factor increases the rate of hepatocyte uptake of human plasma high-density lipoprotein cholesterol. *Biochemistry.* **49**, 9866–9873
21. Rosales, C., Tang, D., Gillard, B. K., Courtney, H. S., and Pownall, H. J. (2011) Apolipoprotein E mediates enhanced plasma high-density lipoprotein cholesterol clearance by low-dose streptococcal serum opacity factor via hepatic low-density lipoprotein receptors in vivo. *Arterioscler. Thromb. Vasc. Biol.* **31**, 1834–1841
22. Rigotti, A., Trigatti, B. L., Penman, M., Rayburn, H., Herz, J., and Krieger, M. (1997) A targeted mutation in the murine gene encoding the high density lipoprotein (HDL) receptor scavenger receptor class B type I reveals its key role in HDL metabolism. *Proc. Natl. Acad. Sci. U. S. A.* **94**, 12610–12615
23. Van Eck, M., Twisk, J., Hoekstra, M., Van Rij, B. T., Van der Lans, C. A., Bos, I. S., *et al.* (2003) Differential effects of scavenger receptor BI deficiency on lipid metabolism in cells of the arterial wall and in the liver. *J. Biol. Chem.* **278**, 23699–23705
24. Ma, K., Forte, T., Otvos, J. D., and Chan, L. (2005) Differential additive effects of endothelial lipase and scavenger receptor-class B type I on high-density lipoprotein metabolism in knockout mouse models. *Arterioscler. Thromb. Vasc. Biol.* **25**, 149–154
25. Liu, J., Gillard, B. K., Yelamanchili, D., Gotto, A. M., Jr., Rosales, C., and Pownall, H. J. (2021) High free cholesterol bioavailability drives the tissue pathologies in Scarb1(-/-) mice. *Arterioscler. Thromb. Vasc. Biol.* **41**, e453–e467
26. Pownall, H. J., Rosales, C., Gillard, B. K., and Gotto, A. M., Jr. (2021) High-density lipoproteins, reverse cholesterol transport and atherogenesis. *Nat. Rev. Cardiol.* **18**, 712–723
27. Lange, Y., and Steck, T. L. (2008) Cholesterol homeostasis and the escape tendency (activity) of plasma membrane cholesterol. *Prog. Lipid Res.* **47**, 319–332
28. Abrams, M. E., Johnson, K. A., Radhakrishnan, A., and Alto, N. M. (2020) Accessible cholesterol is localized in bacterial plasma membrane protrusions. *J. Lipid Res.* **61**, 1538
29. Chakrabarti, R. S., Ingham, S. A., Kozlitina, J., Gay, A., Cohen, J. C., Radhakrishnan, A., *et al.* (2017) Variability of cholesterol accessibility in human red blood cells measured using a bacterial cholesterol-binding toxin. *Elife.* **6**, e23355
30. Steck, T. L., and Lange, Y. (2023) Is reverse cholesterol transport regulated by active cholesterol? *J. Lipid Res.* **64**, 100385

31. Lange, Y., and Steck, T. L. (2020) Active cholesterol 20 years on. *Traffic.* **21**, 662–674
32. Lange, Y., Tabei, S. M. A., and Steck, T. L. (2023) A basic model for the association of ligands with membrane cholesterol: application to cytolysin binding. *J. Lipid Res.* **64**, 100344
33. Braun, A., Trigatti, B. L., Post, M. J., Sato, K., Simons, M., Edelberg, J. M., *et al.* (2002) Loss of SR-BI expression leads to the early onset of occlusive atherosclerotic coronary artery disease, spontaneous myocardial infarctions, severe cardiac dysfunction, and premature death in apolipoprotein E-deficient mice. *Circ. Res.* **90**, 270–276
34. Braun, A., Zhang, S., Miettinen, H. E., Ebrahim, S., Holm, T. M., Vasile, E., *et al.* (2003) Probucol prevents early coronary heart disease and death in the high-density lipoprotein receptor SR-BI/apolipoprotein E double knockout mouse. *Proc. Natl. Acad. Sci. U. S. A.* **100**, 7283–7288
35. Meurs, I., Hoekstra, M., van Wanrooij, E. J., Hildebrand, R. B., Kuiper, J., Kuipers, F., *et al.* (2005) HDL cholesterol levels are an important factor for determining the lifespan of erythrocytes. *Exp. Hematol.* **33**, 1309–1319
36. Holm, T. M., Braun, A., Trigatti, B. L., Brugnara, C., Sakamoto, M., Krieger, M., *et al.* (2002) Failure of red blood cell maturation in mice with defects in the high-density lipoprotein receptor SR-BI. *Blood.* **99**, 1817–1824
37. Hoekstra, M. (2020) Identification of scavenger receptor BI as a potential screening candidate for congenital primary adrenal insufficiency in humans. *Am. J. Physiol. Endocrinol. Metab.* **319**, E102–E104
38. Guo, L., Zheng, Z., Ai, J., Howatt, D. A., Mittelstadt, P. R., Thacker, S., *et al.* (2014) Scavenger receptor BI and high-density lipoprotein regulate thymocyte apoptosis in sepsis. *Arterioscler. Thromb. Vasc. Biol.* **34**, 966–975
39. Miettinen, H. E., Rayburn, H., and Krieger, M. (2001) Abnormal lipoprotein metabolism and reversible female infertility in HDL receptor (SR-BI)-deficient mice. *J. Clin. Invest.* **108**, 1717–1722
40. Yesilaltay, A., Dokshin, G. A., Busso, D., Wang, L., Galiani, D., Chavarria, T., *et al.* (2014) Excess cholesterol induces mouse egg activation and may cause female infertility. *Proc. Natl. Acad. Sci. U. S. A.* **111**, E4972–E4980
41. Yesilaltay, A., Morales, M. G., Amigo, L., Zanlungo, S., Rigotti, A., Karackattu, S. L., *et al.* (2006) Effects of hepatic expression of the high-density lipoprotein receptor SR-BI on lipoprotein metabolism and female fertility. *Endocrinology.* **147**, 1577–1588
42. Rosales, C., Yelamanchili, D., Gillard, B. K., Liu, J., Gotto, A. M., Jr., and Pownall, H. J. (2023) Serum opacity factor rescues fertility among female Scarbl(-/-) mice by reducing HDL-free cholesterol bioavailability. *J. Lipid Res.* **64**, 100327
43. Radin, N. S. (1981) Extraction of tissue lipids with a solvent of low toxicity. *Methods Enzymol.* **72**, 5–7
44. Havel, R. J., Eder, H. A., and Bragdon, J. H. (1955) The distribution and chemical composition of ultracentrifugally separated lipoproteins in human serum. *J. Clin. Invest.* **34**, 1345–1353
45. Schumaker, V. N., and Puppione, D. L. (1986) Sequential flotation ultracentrifugation. *Methods Enzymol.* **128**, 155–170
46. Lund-Katz, S., Hammerschlag, B., and Phillips, M. C. (1982) Kinetics and mechanism of free cholesterol exchange between human serum high- and low-density lipoproteins. *Biochemistry.* **21**, 2964–2969
47. Davidson, W. S., Heink, A., Sexmith, H., Melchior, J. T., Gordon, S. M., Kuklenyik, Z., *et al.* (2016) The effects of apolipoprotein B depletion on HDL subspecies composition and function. *J. Lipid Res.* **57**, 674–686
48. Xu, B., Gillard, B. K., Gotto, A. M., Jr., Rosales, C., and Pownall, H. J. (2017) ABCA1-Derived nascent high-density lipoprotein-apolipoprotein AI and lipids metabolically segregate. *Arterioscler. Thromb. Vasc. Biol.* **37**, 2260–2270
49. Schwartz, C. C., VandenBroek, J. M., and Cooper, P. S. (2004) Lipoprotein cholesteryl ester production, transfer, and output in vivo in humans. *J. Lipid Res.* **45**, 1594–1607
50. de Boer, J. F., Schonewille, M., Dikkers, A., Koehorst, M., Havinga, R., Kuipers, F., *et al.* (2017) Transintestinal and biliary cholesterol secretion both contribute to macrophage reverse cholesterol transport in rats-brief report. *Arterioscler. Thromb. Vasc. Biol.* **37**, 643–646
51. Picardo, M., Massey, J. B., Kuhn, D. E., Gotto, A. M., Jr., Gianturco, S. H., and Pownall, H. J. (1986) Partially reassembled high density lipoproteins. Effects on cholesterol flux, synthesis, and esterification in normal human skin fibroblasts. *Arteriosclerosis.* **6**, 434–441
52. Dole, V. S., Matuskova, J., Vasile, E., Yesilaltay, A., Bergmeier, W., Bernimoulin, M., *et al.* (2008) Thrombocytopenia and platelet abnormalities in high-density lipoprotein receptor-deficient mice. *Arterioscler. Thromb. Vasc. Biol.* **28**, 1111–1116
53. Li, X. M., Tang, W. H., Mosior, M. K., Huang, Y., Wu, Y., Matter, W., *et al.* (2013) Paradoxical association of enhanced cholesterol efflux with increased incident cardiovascular risks. *Arterioscler. Thromb. Vasc. Biol.* **33**, 1696–1705
54. Devaux, P. F. (1991) Static and dynamic lipid asymmetry in cell membranes. *Biochemistry.* **30**, 1163–1173
55. Op den Kamp, J. A. (1979) Lipid asymmetry in membranes. *Annu. Rev. Biochem.* **48**, 47–71
56. Verkleij, A. J., Zwaal, R. F., Roelofsen, B., Comfurius, P., Kastelijn, D., and van Deenen, L. L. (1973) The asymmetric distribution of phospholipids in the human red cell membrane. A combined study using phospholipases and freeze-etch electron microscopy. *Biochim. Biophys. Acta.* **323**, 178–193
57. Schick, P. K., Kurica, K. B., and Chacko, G. K. (1976) Location of phosphatidylethanolamine and phosphatidylserine in the human platelet plasma membrane. *J. Clin. Invest.* **57**, 1221–1226
58. Sandra, A., and Pagano, R. E. (1978) Phospholipid asymmetry in LM cell plasma membrane derivatives: polar head group and acyl chain distributions. *Biochemistry.* **17**, 332–338
59. Bollen, I. C., and Higgins, J. A. (1980) Phospholipid asymmetry in rough- and smooth-endoplasmic-reticulum membranes of untreated and phenobarbital-treated rat liver. *Biochem. J.* **189**, 475–480
60. Lorent, J. H., Levental, K. R., Ganesan, L., Rivera-Longsworth, G., Sezgin, E., Doktorova, M., *et al.* (2020) Plasma membranes are asymmetric in lipid unsaturation, packing and protein shape. *Nat. Chem. Biol.* **16**, 644–652
61. Liu, S. L., Sheng, R., Jung, J. H., Wang, L., Stec, E., O'Connor, M. J., *et al.* (2017) Orthogonal lipid sensors identify transbilayer asymmetry of plasma membrane cholesterol. *Nat. Chem. Biol.* **13**, 268–274
62. Hamilton, J. A. (2003) Fast flip-flop of cholesterol and fatty acids in membranes: implications for membrane transport proteins. *Curr. Opin. Lipidol.* **14**, 263–271
63. Niu, S. L., and Litman, B. J. (2002) Determination of membrane cholesterol partition coefficient using a lipid vesicle-cyclodextrin binary system: effect of phospholipid acyl chain unsaturation and headgroup composition. *Biophys. J.* **83**, 3408–3415
64. Homan, R., and Pownall, H. J. (1988) Transbilayer diffusion of phospholipids: dependence on headgroup structure and acyl chain length. *Biochim. Biophys. Acta.* **938**, 155–166
65. Kayden, H. J., Silber, R., and Kossmann, C. E. (1965) The role of vitamin E deficiency in the abnormal autohemolysis of acanthocytosis. *Trans. Assoc. Am. Physicians.* **78**, 334–342
66. Wetterau, J. R., Aggerbeck, L. P., Bouma, M. E., Eisenberg, C., Munck, A., Hermier, M., *et al.* (1992) Absence of microsomal triglyceride transfer protein in individuals with abetalipoproteinemia. *Science.* **258**, 999–1001
67. Ways, P., Reed, C. F., and Hanahan, D. J. (1963) Red-cell and plasma lipids in acanthocytosis. *J. Clin. Invest.* **42**, 1248–1260
68. Tziakas, D. N., Kaski, J. C., Chalikias, G. K., Romero, C., Fredericks, S., Tentes, I. K., *et al.* (2007) Total cholesterol content of erythrocyte membranes is increased in patients with acute coronary syndrome: a new marker of clinical instability? *J. Am. Coll. Cardiol.* **49**, 2081–2089